COMPRESSOR RESPONSE TO SYNCHRONOUS MOTOR STARTUP

by

Gerald K. Mruk

Analytical Engineer

Joy Manufacturing Company

Buffalo, New York

Gerald K. Mruk is an analytical engineer for Joy Manufacturing Company, performing analysis of lateral and torsional vibration in centrifugal compressor pinions and drive shaft systems. He has been active in correlating analytical results with field data in numerous troubleshooting and problem diagnosis situations. Mr. Mruk has published ASME papers and authored trade magazine articles in his present area of interest.

Previously he was employed as a research engineer by Cornell Aeronautical Laboratory where he was engaged in modeling radar acquisition systems and in conducting wind tunnel tests.

Mr. Mruk graduated from Rensselaer Polytechnic Institute and earned an M.S.E. from Princeton University.

ABSTRACT

Synchronous machines produce an oscillating torque at twice slip frequency on starting. If the shaft system of a coupled compressor is not adequately designed, or if the motor malfunctions, this torsional excitation will have destructive effect. Recently, mathematical models for this sytem have been solved by direct integration on both analog and digital computers. Important aspects of the model include: representation of the electrical power feed network for the motor, an equivalent circuit description of the motor itself, and a non-linear characterization of the shafts and couplings connecting the compressors to the motor.

In parallel with this analytical effort it was recognized that the instantaneous magnitude of the excitation torque and its resultant shaft stress should be measured during field installation. In order to accomplish this, a torsional acceleration monitor, which is attached to the uncoupled synchronous motor, was developed to gauge the actual torques being applied to the compressor on startup. In addition, a strain measurement system utilizing telemetry was assembled to obtain shaft stress levels. These two instrumentation packages have been used to insure safe operation, detect motor starting malfunctions, and verify the analytical design of the shaft/coupling system. Measurements have been made at 10 installations to date with good agreement between expected and experienced results.

INTRODUCTION

Synchronous motors present centrifugal compressor manufacturers with a problem unique among the various drivers available for their machinery. This problem is one of torsional response to pulsating torques generated by salient pole motors upon starting. These torques, if adequate safeguards are not taken, can be severe enough to cause failure of keys, couplings, and shafts. Fortunately, the information required to protect coupled machinery is available to the engineers responsible for integrating the compressor with its motor, and accounting for their combined operation within a power distribution network. Two elements are necessary to thoroughly perform this task.

First, rigorous analysis must be done at the design stage of the equipment. A suitable approach is to model the electric motor with enough detail so that both the two times slip frequency torque and the motor average torque are directly calculated. The pulsating torque produced during starting results from the asymmetry of the synchronous motor rotor and so a two axis representation of the machine permits development of a system of differential equations which have non-symmetric coefficients. Of course, the motor is tied into a distribution network involving power company equipment as well as operating plant transformers and cables. This power system is modeled through an equivalent circuit arrived at by transforming the significant elements in accordance with Thevenin's theorem. The electrical torque resulting from this analysis is the excitation that is applied to the compressor shafting. An important advantage to developing the excitation in this detailed manner is that acceleration effects are explicitly addressed, obviating the need for assumptions as to how load acceleration will influence vibrations in the mechanical system. The mechanical system of interest is comprised of compressors, couplings and shafts. It is straightforwardly described by second order differential equations which have provisions for non-linear terms to represent resilient couplings.

Second, measurements must be made of the actual excitation being applied to the compressor shafts during field startups. The instrumentation used has to be carefully designed so that the twice slip frequency torques are clearly identifiable from a background of potentially large amplitude signals. The interfering frequencies can be especially strong at instantaneous running speed and at any instrumentation system resonance. A torsional acceleration monitor was designed, constructed, and used to measure the torque output of several synchronous motors during the installation period and prior to compressor coupling. In addition, it is important that the response to this excitation be measured. Instrumentation adequate for this purpose is conventional strain gaging with signals brought off the rotating shafts by telemetry.

MATHEMATICAL MODEL

This section shows how the equations describing the power distribution network, the salient pole motor, and the compressor are coupled. Furthermore, it indicates the choices of available solution techniques and gives illustrative examples.

Power System One-Line Diagram

The three-phase synchronous motor armature is paralleled through an equivalent distribution system impedance to a utility with high generating capacity, as indicated in Figure 1. In
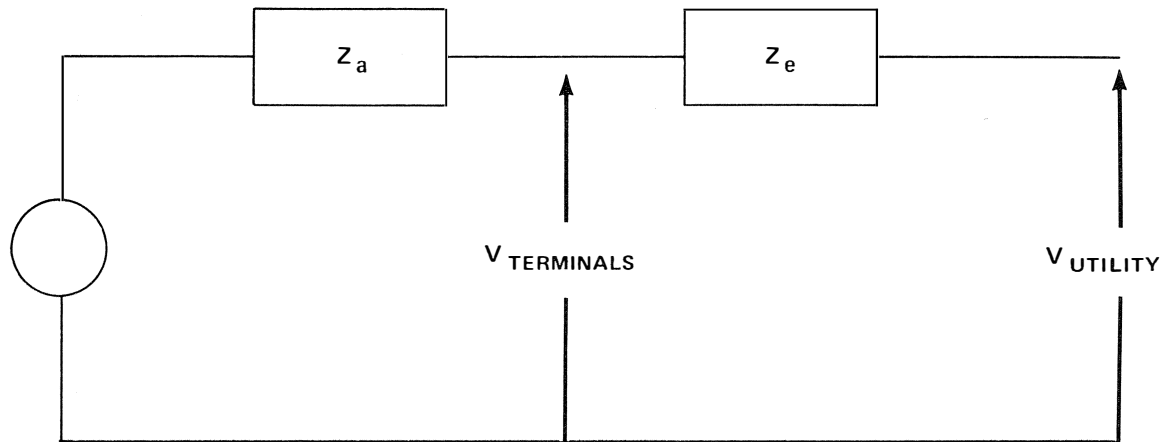
Figure 1. Utility-Motor Equivalent Circuit.

this diagram, Ze is the Thevenin's equivalent impedance looking from the machine's terminals. It generally includes overhead lines, transformers and cables between the utility and the motor. An illustrative one-line diagram for a distribution network is shown in Figure 2. The equivalent impedance is easily calculated in per unit terms on the motor kVa base from this diagram. For example, given the short-circuit kVA for the utility and using the fact that the per unit impedance of the utility on its own kVA base is 1.0, the desired per unit impedance for use in computing Ze is:

$$\frac{1.0 \times \text{motor kVA base}}{\text{Utility short-circuit kVA}}$$

If the utility generator's X/R is known then this impedance can be broken down into reactance and resistance. If the lengths of lines and cables as well as the specific types are known, then handbook data will give reasonable estimates for impedance in ohms. These are converted to the per unit system through normalization by the base impedance for the motor. Transformer characteristics are given in percent of transformer rating kVA base and X/R; therefore, conversion to the motor base is also required. The sum of these elements yields the equivalent impedance of Figure 1.

Synchronous Motor

There are many computer simulations of synchronous machines described in the open literature. A convenient analysis uses the two-axis theory of the synchronous machine, which permits the motor to be described by the equivalent circuits shown in Figure 3. This is a lumped parameter model of the machine in which non-linear effects, such as hysteresis and saturation, are ignored. A detailed analysis results in six first order differential equations [1] in terms of currents and flux linkages. The coefficients of this system of equations are functions of the parameters shown in the equivalent circuit, and also line frequency and motor speed. The resistances and reactances used in the equivalent circuits are all readily available from the motor manufacturers. However, caution must be exercised in interpreting the supplied information, as there appears to be no uniformly accepted nomenclature. For example, X_{md} in this presentation is the direct axis magnetizing reactance representing the inductive coupling of the rotor and armature. Some manufacturers designate this quantity, X_{ad}, the direct axis armature reactance. Since the concern here is with start-up torques, it is also important to consider the field resistance, R_f, to include any field discharge resistor resistance supplied with the motor. In addition, it is noted that the equiv-
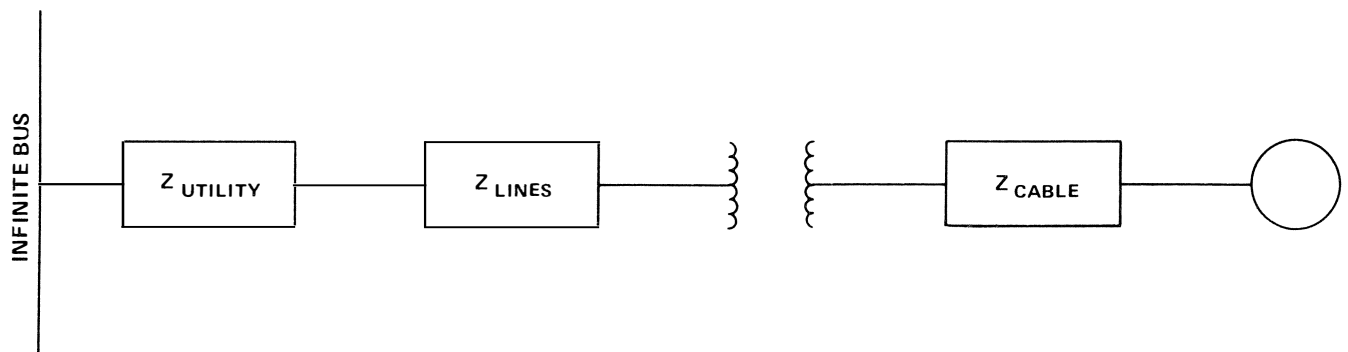

Figure 2. One-Line Diagram.

alent circuit parameters may vary with slip frequency. For this reason, the motor manufacturer should be advised of the intended use so that appropriate values are supplied.

Per-unit quantities are used in the distribution system model, and also here in the state equations for the synchronous motor. This is of considerable advantage in analog computer solutions to the system of differential equations, in that the equivalent circuit constants lie in a reasonably narrow range and, therefore, rescaling of the analog computer (a time-consuming process) is minimized. Per-unit quantities are ratios of physical quantities to appropriately chosen base quantities. The following list gives both electrical and mechanical base quantities.

Voltage = rated phase voltage − V_B (v)

Current = rated phase current − I_B (amp)

Impedance = $\dfrac{V_B}{I_B}$ (ohms)

Power = rated input volt amperes = $3V_BI_B$ (watts)

Flux linkage = V_B − λ_B (weber-turns)

Speed = rated synchronous speed − v_B (rad/sec)

Torque = motor rated torque = Rated H.P./Rated rpm × 5250 − T_B (ft-lbs).

Compressors and Couplings

The mechanical system model is illustrated in Figure 4. Its equations of motion are linked to the system of equations representing the electric motor through the motor speed and air gap torque. Equations of motion for this system result in the following state description:

DIRECT AXIS

QUADRATURE AXIS

Figure 3. Two-Axis Equivalent Circuits.

$$\frac{dv_0}{dt} + \frac{B_0}{J_0}(v_0 - v_1) + \frac{K_0}{J_0}(\Theta_0 - \Theta_1) = \frac{T_B}{J_0 v_B} T_e$$

$$\frac{dv_1}{dt} + \frac{B_0}{J_1}(v_1 - v_0) + \frac{B_1}{J_1}f_{TDP}(\Delta\Theta_{12})(v_1 - v_2) + \frac{K_0}{J_1}(\Theta_1 - \Theta_0) + \frac{T_1}{J_1 v_B}f_{TD}(\Delta\Theta_{12}) = 0$$

$$\frac{dv_2}{dt} + \frac{B_1}{J_2}f_{TDP}(\Delta\Theta_{21})(v_2 - v_1) + \frac{B_2}{J_2}(v_2 - v_3) + \frac{T_1}{J_2 v_B}f_{TD}(\Delta\Theta_{21}) + \frac{K_2}{J_2}(\Theta_2 - \Theta_3) = 0$$

$$\frac{dv_3}{dt} + \frac{B_2}{J_3}(v_3 - v_2) + \frac{B_3}{J_3}(v_3 - v_4) + \frac{K_2}{J_3}(\Theta_3 - \Theta_2) + \frac{K_3}{J_3}(\Theta_3 - \Theta_4) = \frac{T_3}{v_B J_3}f_{TS}(v_3)$$

$$\frac{dv_4}{dt} + \frac{B_3}{J_4}(v_4 + v_3) + \frac{B_4}{J_4}f_{TDP}(\Delta\Theta_{45})(v_4 - v_5) + \frac{K_3}{J_4}(\Theta_4 - \Theta_3) + \frac{T_4}{J_4 v_B}f_{TD}(\Delta\Theta_{45}) = 0$$

$$\frac{dv_5}{dt} + \frac{B_4}{J_5}f_{TDP}(\Delta\Theta_{54})(v_5 - v_4) + \frac{B_5}{J_5}(v_5 - v_6) + \frac{T_4}{J_5 v_B}f_{TD}(\Delta\Theta_{54}) + \frac{K_5}{J_5}(\Theta_5 - \Theta_6) = 0$$

$$\frac{dv_6}{dt} + \frac{B_5}{J_6}(v_6 - v_5) + \frac{K_5}{J_6}(\Theta_6 - \Theta_5) = \frac{T_6}{v_B J_6}f_{TS}(v_6)$$
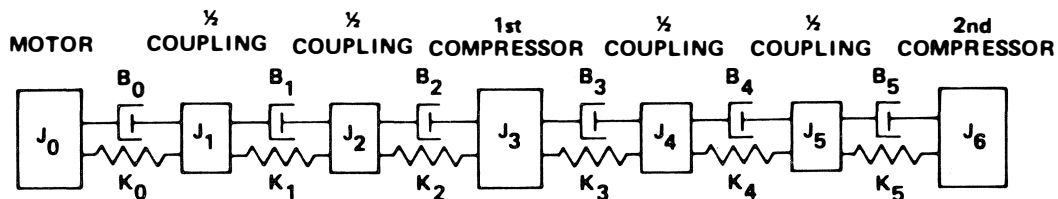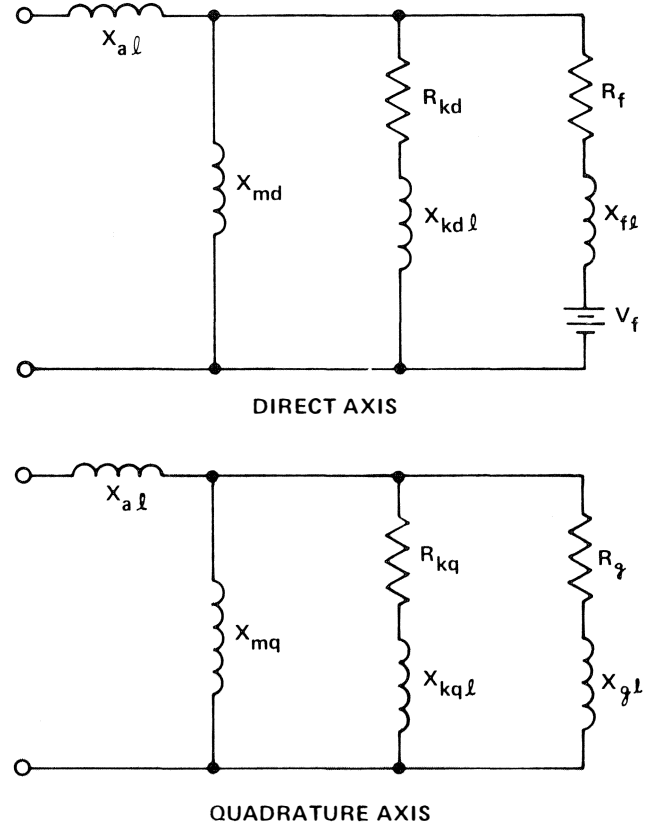

Figure 4. Mass-Elastic System.

These equations take the springs and dampers at stations 1 and 4 to be nonlinear, and so allow modeling of flexible resilient couplings which have the characteristic shown in Figure 5. The terms on the right-hand side of the compressor equations represent load torques during starting and are modeled by the curve of Figure 6.

The complications do not arise when modeling linear couplings, and the equations simplify to have constant coefficients. Several arrangements of the mass-elastic system components are of practical interest. The systems that have been modeled are schematically shown in Figure 7. The top two diagrams represent linear systems with the motor driving one or two compressors. The remaining diagrams illustrate possible placement positions of either a single non-linear coupling or two non-linear couplings.

Solution Techniques

The equations described above have been solved both on analog and digital computers. The analog equipment consisted of three EAI-380 computers (Electronic Associate, Inc.). These machines have double-pole, double-throw function switches, enabling all of the modeled systems to be permanently wired. The appropriate set of equations for a particular study is selected by positioning the switches properly. These computers also have servo multipliers to generate the necessary products of terms and non-linearities, as well as resolvers to produce trigonometric functions. The completed system required 73 amplifiers (integrators, summers, and inverters), 18 servo multipliers and 91 attenuators. The solution was patched such that the equations describing the synchronous motor are solved on one of the computers, the non-linear portion of the mechanical system on a second computer and the linear part of the mechanical system on a third.

The analog solution has two notable advantages. First, because variables are continuously generated, there is no problem in the stability of the non-linear cases. This contrasts with digital computer results where solutions have numerical instabilities if integration step sizes are not carefully chosen. Second, after the initial programming costs, the cost per run is not strongly dependent on the complexity of the mechanical system or the number of output plots generated. However, there are significant limitations. Because the problem involves high frequencies over long periods of time, amplifier instabilities cause run-to-run non-repeatability in the state variables of the synchronous motor and, therefore, in the air gap torque. Several attempts were made to control amplifier drift rates, including the use of a second analog computer (COMCOR, Inc. Ci-5000), but this problem could not be eliminated. Another problem area is the difficulty in detecting and preventing operator errors. This condition exists because attenuators are set and minor scaling changes are made from problem-to-problem while the computer does not furnish a hard copy of run setups. Although a Hybrid analog computer would eliminate this consideration with respect to attenuator settings, it could not improve the situation as regards scaling changes.

Because of these problems, the system of equations was also solved digitally on an IBM 370/168. Again, all of the different compressor systems modeled are simulated through the use of different subroutines for the various mass-elastic systems. The program uses 500 K Bytes of core storage and CPU times vary from about 30 seconds for a simple system (Figure 7a, 4 second start-up time) to about 600 seconds for a case involving two compressors, resilient couplings, and a lengthy start-up time (Figure 7e, 12 seconds start). The differential equations have been solved using both a forth-order Runge-Kutta method coded in double precision and a variable step

predictor-corrector method (Adams-Moulton). The variable step technique results in much shorter processing times than noted above, but the plotted results do not display all of the higher frequency details. The outputs are both in the form of tables containing maximum, minimum, and average values of motor speed, air gap torque, and shaft torques over tenth second intervals and in the form of plots of speed and torque versus time.
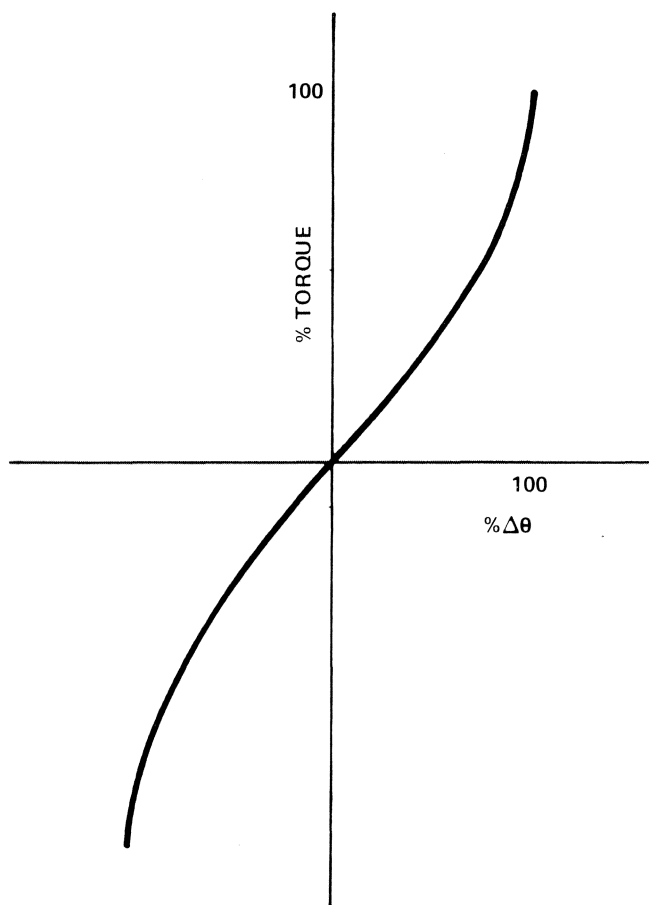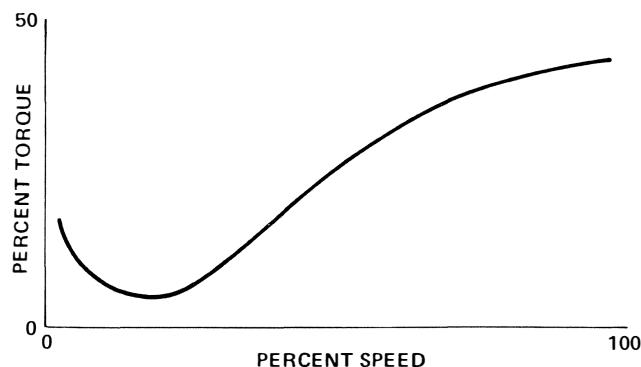

Figure 5. Nonlinear Coupling Characteristics.

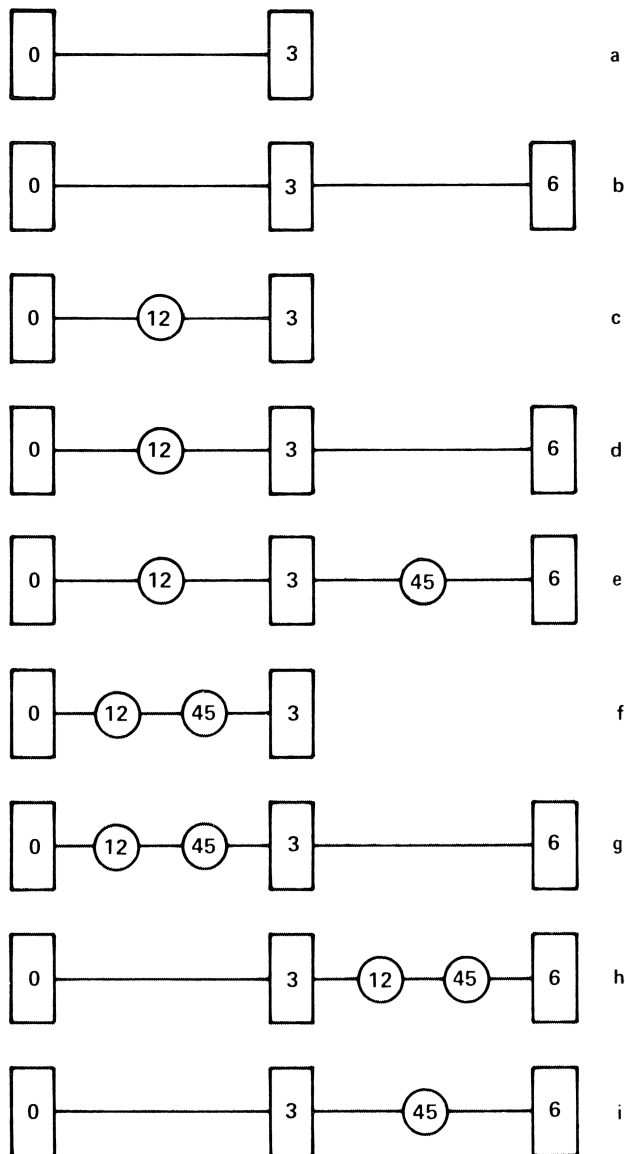
Figure 6. Compressor Load Characteristics.

Figure 7. Mechanical Systems Modeled.

starting. Referring to the mass-elastic equations previously given, it is seen that in this case the air gap torque works only on the polar inertia of the motor rotor. For this reason, measuring instantaneous values of motor rotor acceleration when started alone results in a direct measure of the torque available for system excitation.

The system described here for measuring instantaneous motor angular acceleration consists of the attachment of two opposing accelerometers mounted at equal radii on a disk. This assembly, shown in Figure 8, is fastened to the end of the motor rotor. The outputs from these accelerometers are summed to cancel the once per revolution gravitational effect on each accelerometer. It should also be noted that this summation results in a doubling of sensitivity to angular acceleration.

A major concern in building and using this instrument is minimization of the very large radial component of acceleration felt by each accelerometer. The desire is to accurately measure torsional acceleration only. The radial component will give unwanted output unless the accelerometers have a low transverse sensitivity, and, further, unless each accelerometer is mounted so that its zero cross axis is radial. Good results have been obtained when a shaker table was used to define the cross axis sensitivity of the accelerometers as a function of their angular orientation.

The design of Figure 8 will measure the two times slip frequency oscillatory torques of a synchronous motor as it accelerates, uncoupled, to rated speed. If accelerometers with large time constants are chosen, the low frequency oscillations near full speed will be well defined, and, also, the change of average acceleration rate will be shown by the data. Figure 9 shows a schematic output of the accelerometers used on a motor with increasing acceleration rate to speed. It is interesting to note that the amount of drop area A_1 and overshoot area A_2 are functions of the accelerometer time constant and may be factored out of the data if desired.

Figure 8 illustrates the complete mechanical and electrical arrangement of the torsional acceleration measurement system. In addition to the components previously described, two constant current diodes are required for proper operation. These diodes insure constant accelerometer sensitivity over a range of batter voltages. The tape recorder allows data to be
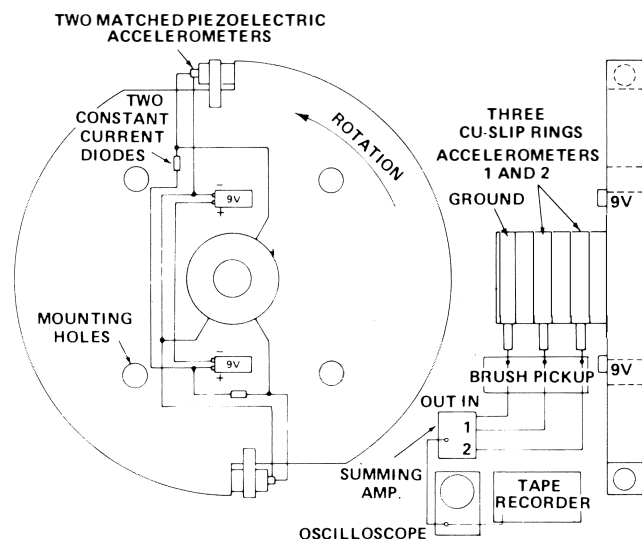
INSTRUMENTATION AND MEASUREMENTS

The material presented here is intended to describe a device that has been designed, fabricated, and used for the measurement of synchronous motor output torques. Actual measured data is shown as well as response data determined by strain gages.

Air Gap Torques

Motor inrush wattage has been used by others for field measurement of synchronous motor developed torques. However, that method has met with controversy because it has not considered the losses internal to the motor during starting. In a number of cases, this procedure has led to a good measure of average motor air gap torque, but to an understating of the amplitudes of air gap torque fluctuation. This has led to a lack of correlation with the driven system's estimated response.

It is believed that the pulsating portion of synchronous motor air gap torque can best be measured upon solo motor

Figure 8. Torsional Acceleration Monitor.

obtained in real time and later analyzed at reduced tape speeds.

Shaft Strain

Having measured the torsional excitation, a complete set of field data requires measurement of the response of the driven system to that excitation. This data is readily obtained as shaft strain and is conventionally recorded through the use of slip rings or telemetry instrumentation. The shaft torque data presented here was acquired by means of a telemetry system similar to that shown in Figure 10.

COMPARISON OF SIMULATED AND MEASURED DATA

Figures 11, 12(a) and 13(b) are, respectively, a system simulated start-up, air gap torque field data, and shaft torque field data. Figure 12(b) presents the accelerometer system output at motor rated speed. The lack of output indicates proper elimination of the gravitational effect. Figure 12(c), also obtained at full speed, shows the output of one accelerometer. The amplitude of this trace indicates ± 1 g voltage levels. Figure 13(a) is a tachometer signal obtained from a proximiter probe viewing the rotation of metallic tape mounted on the driver shaft, recorded simultaneously with shaft stress. The system simulated and tested was a two-tandem compressor installation driven by an 1800-rpm synchronous motor, so that two distinct torsional resonances were present.
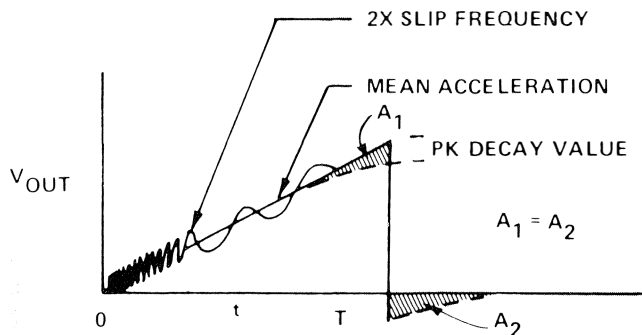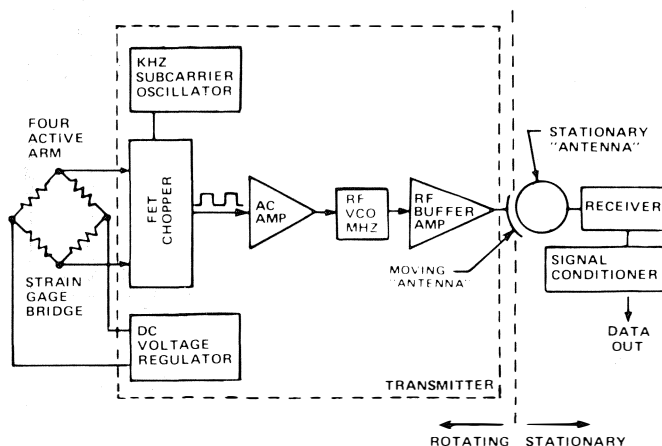
The principal evaluations made from Figures 11, 12, and 13 are:

1. A major amplitude line frequency torsional burst occurs at the first moments of start-up as predicted by the simulation. This, again, demonstrates that no motor driven system should be designed with torsional resonances near line frequency or two times line frequency.

2. In the upper speed ranges where torsional resonances will be excited, the air gap torque peak to peak oscillation measures at 0.7 to 0.8 per unit which correlates well with the simulation predicted excitation. The motor used for these tests is a four-pole, solid rotor design.

3. Peak air gap torque is slightly higher than the simulation results, due to a higher-than-predicted average air gap torque.

4. The shaft torque data shows the response of the system to the initial line frequency burst from the motor and a decaying of that step input at the system's fundamental resonant frequency.
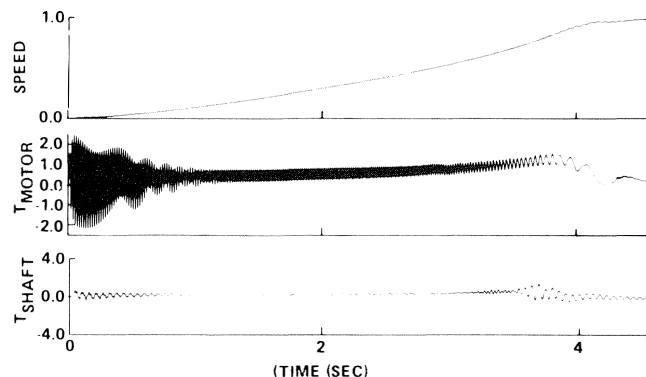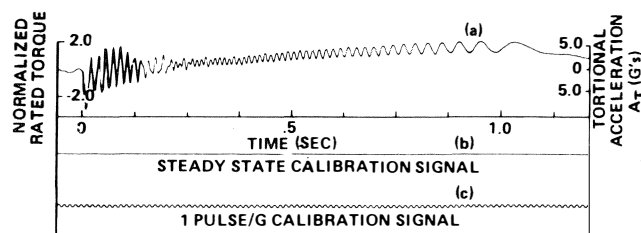
Figure 11. Simulation of Start-up.

Figure 9. Terminated Sawtooth Ramp with Superimposed Double Slip Frequency.

Figure 12. Measured Air Gap Torque During Start-up.

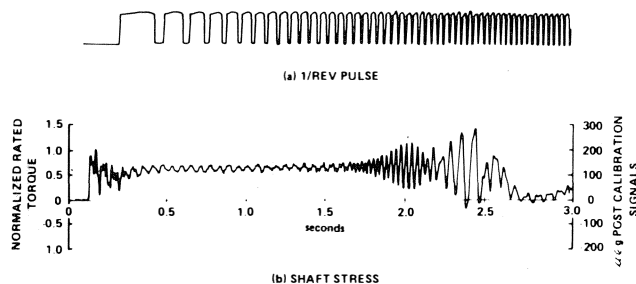*Figure 10. Shaft Strain Measurement System.*

Figure 13. Measured Main Drive Shaft Stress During Start-up.

5. The shaft torque data shows distinctly the two resonant torsional frequencies of the system.

6. Peak shaft torque occurs during the fundamental mode of torsional vibration and peaks at 1.6 per unit as predicted by the simulation.

7. Predicted starting times are considerably longer than field data shows. This is caused by a larger-than-predicted average torque. The use of constant electrical characteristics is believed to be the cause of this discrepancy, especially in the lower 50 percent speed range. As mentioned in Reference 1, the electrical characteristics of the motor should be chosen to be correct near the speed of resonance. This will provide good prediction capabilities in the region of resonance, which is the prime concern. Accurate prediction of starting time is not an aim of this paper, but could probably be improved by the use of frequency-dependent electrical characteristics.

NOMENCLATURE

B = damping coefficient
J = inertia
K = spring rate

Subscripts

0 = motor
1 = nonlinear coupling half

R = resistance
t = time
T = torque
V = voltage
X = reactance
Z = impedance
Θ = per unit angular displacement
v = per unit speed

2 = nonlinear coupling half
3 = compressor
4 = nonlinear coupling half
5 = nonlinear coupling half
6 = compressor
B = base quantity
d = direct axis

e = air gap, equivalent
f = field
g = additional solid pole damper
k = cage
q = quadrature axis

REFERENCES

1. Mruk, G., Halloran, J., and Kolodziej, R., "Torsional Response of Compressor Shaft Systems During Synchronous Motor Startup," Part I - Analytical Model ASME Paper 77-Pet-49, Part II - Field Measurement Techniques ASME Paper 77-Pet-60 and Part III - Abnormal Motor Conditions ASME Paper 77-Pet-56.